Wideband Photonic Microwave Frequency Divider With Large Harmonic Suppression Capability

Hao Chen, *Member, IEEE*, and Erwin H. W. Chan, *Senior Member, IEEE*

***Abstract*—An all-optical photonic microwave frequency divider (PMFD) is presented. It is based on injecting an RF phase modulated optical signal into a semiconductor laser oscillating in the period-two state. New optical frequency components with frequency separation of half of the input RF signal frequency are generated at the laser output. A frequency divided signal can be obtained by the beating of these optical frequency components at a photodetector. Large harmonic suppression can be achieved by using an optical filter to select only two optical frequency components to be detected by the photodetector. The proposed PMFD is free of electrical components and does not suffer from the modulator bias drift problem. It has the potential to operate over a 100 GHz frequency range. System parameters required to realise divide-by-two frequency division operation for different input RF signal frequencies are investigated. Experimental results are presented for the novel PMFD, which demonstrate the generation of a 1/2 frequency component for different input RF signal frequencies by controlling the forward bias current of an off-the-shelf semiconductor laser, and which also show the important advantages of large harmonic suppression and high signal-to-noise ratio performance. Wide input RF signal power range and high output stability performance are also demonstrated experimentally.**

***Index Terms*—Frequency division, microwave photonics, optical injection, optical signal processing, semiconductor laser.**

I. Introduction

MANY applications including telecommunication, defence, astronomy, instrumentation, and healthcare require altering the frequency of an RF signal [1]–[5]. The signal processors, which perform this function, are frequency mixers, frequency shifters, frequency multipliers and frequency dividers. Numerous microwave photonic techniques to implement these signal processors have been reported. This arises from the potential of wide bandwidth, immunity to electromagnetic interference (EMI) and integrability, in microwave photonics [4], [5]. Compared to mixers and multipliers, there are less than 20 reports on photonic microwave frequency dividers (PMFDs). Among them, majority are based on the regenerative technique or the injection locking technique implemented using an optoelectronic oscillator (OEO) loop [6]–[11]. The operating frequency range of these OEO based PMFDs is limited by the bandwidth of the electrical components such as microwave amplifier, phase shifter, bandpass filter and power splitter used in the structure. PMFDs can also be implemented based on the nonlinear effect in a semiconductor optical amplifier (SOA) [12], [13]. However, the operating frequency range of these PMFDs is limited by the SOA lifetime. Furthermore, components such as a dispersive compensating fibre are needed, which increases the system size and prevents the PMFD to be integrated into a compact device.

PMFDs based on nonlinear dynamics of an optically injected semiconductor laser are simple, all-optical and integrable. Until now, there are only three reports on using this technique to implement a frequency divider [14]–[16]. In [14], the semiconductor laser subject to optical injection is directly modulated by an input RF signal whose frequency needs to be divided. It is well known that direct modulation has a limited bandwidth. In [15], the injection light is an externally modulated optical signal from an electro-absorption modulator (EAM) distributed feedback (DFB) laser diode. It is injected into a Fabry-Perot (FP) laser oscillating in period-one state. Since the system that uses an FP laser as an optical source generates high output noise power, the PMFD presented in [15] has very low signal-to-noise ratio (SNR) of only around 25 dB in a 1 MHz noise bandwidth. The PMFD presented in [16] eliminates the drawbacks of limited bandwidth and low SNR performance by using a quadrature biased Mach Zehnder modulator (MZM) for RF signal modulation and injecting the RF intensity modulated optical signal into a DFB laser. In order for the system to be used in practice, a bias controller is required to stabilise the modulator operating point in the transfer function. This is important as changing the modulator bias point alters the injection light power and consequently degrades the PMFD performance. Using a bias controller to lock the modulator bias point increases the system size and complexity. More importantly the output of all three reported optically injected semiconductor laser based PMFDs [14]–[16] consists of high-amplitude harmonic components in addition to the frequency divided signal. The harmonic components need to be suppressed to minimise distortion.

The aim of this paper is to present an optically injected semiconductor laser based PMFD, which has the ability to largely suppress the harmonic components. Furthermore, the input RF signal is applied to an optical phase modulator, which does not require a DC bias voltage. Moreover, the proposed PMFD has a very simple structure, a high SNR and a wide operating frequency range. Experimental results are presented that demonstrates divide-by-two frequency division operation over an 8 to 20 GHz frequency range. Frequency division with

Manuscript received 8 May 2022; revised 22 July 2022; accepted 25 July 2022. Date of publication 1 August 2022; date of current version 10 August 2022. *(Corresponding author: Erwin H. W. Chan.)*

The authors are with the College of Engineering, IT and Environment, Charles Darwin University, Darwin NT 0810, Australia (e-mail: erwin.chan@cdu.edu.au).

Digital Object Identifier 10.1109/JPHOT.2022.3195260

This work is licensed under a Creative Commons Attribution 4.0 License. For more information, see https://creativecommons.org/licenses/by/4.0/

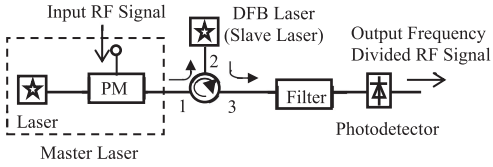

Fig. 1. Proposed photonic microwave frequency divider topology.

over 40 dB harmonic suppression and a 70 dB SNR in a 100 kHz noise bandwidth for a 16 GHz input RF signal, are demonstrated. Results also demonstrate the proposed PMFD exhibits long-term stability and a wide input RF power operating range, which are important properties of a frequency divider but have not been investigated in the reported PMFDs [14]–[16].

II. Topology and Operation Principle

Fig. 1 shows the structure of the proposed optically injected semiconductor laser based PMFD. A laser source generates a continuous wave (CW) light with a frequency f_c. The light is launched into an optical phase modulator (PM) driven by an input RF signal, whose has a frequency f_{RF} that needs to be divided. The phase modulator output electric field can be written as

$$\begin{aligned} E_{o,PM}(t) = E_{in}\sqrt{t_{ff}}e^{j\omega_c t}\big[&J_2(\beta_{RF})\,e^{-j2\omega_{RF}t} \\ &- J_1(\beta_{RF})\,e^{-j\omega_{RF}t} \\ &+ J_0(\beta_{RF}) + J_1(\beta_{RF})\,e^{j\omega_{RF}t} \\ &+ J_2(\beta_{RF})\,e^{j2\omega_{RF}t}\big] \end{aligned} \tag{1}$$

where E_{in} is the electric field amplitude of the CW light into the phase modulator, t_{ff} is the insertion loss of the phase modulator, $J_n(x)$ is the Bessel function of nth order of the first kind, $\omega_c = 2\pi f_c$ and $\omega_{RF} = 2\pi f_{RF}$ are the angular frequency of the optical carrier and the input RF signal respectively, $\beta_{RF} = \pi V_{RF}/V\pi$ is the modulation index, V_{RF} is the input RF signal voltage and $V\pi$ is the phase modulator switching voltage. Note that only the first and second order sidebands are considered in (1). The higher order sidebands are neglected as they have small amplitudes. The blue lines in Fig. 2(a) show the phase modulator output optical spectrum, which consists of an optical carrier and two pairs of RF modulation sidebands. The amplitude and phase of each frequency component generated by the phase modulator are labelled in the figure. The RF phase modulated optical signal is referred to as the injection light from a master laser (ML). It passes through an optical circulator and is injected into a standard off-the-shelf DFB laser, which is referred to as a slave laser (SL). The SL free running frequency f_s is between the carrier and the first order lower sideband of the ML, as shown by the green dashed line in Fig. 2(a).

The SL can be operated at various dynamic states including stable locking, periodic oscillation and chaos, depending on the detuning frequency and the injection strength [17], [18]. The detuning frequency f_i is the difference between the SL free running frequency and the ML frequency. The injection strength ξ is the square root of the ratio of the ML power to

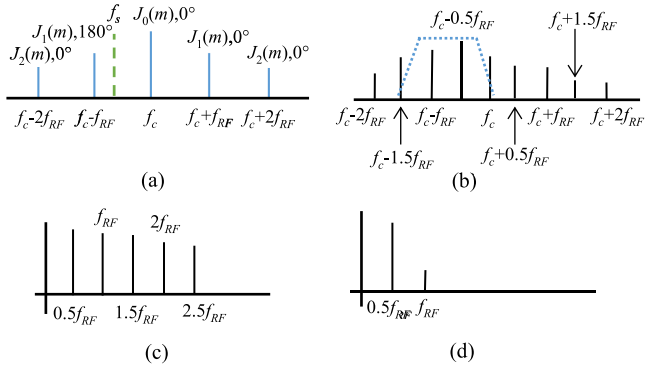

Fig. 2. (a) Optical spectrums of the ML (blue lines) and the free running SL (green dashed line). (b) Output optical spectrum of the SL oscillating in the P2 state. Tunable OBPF magnitude response (blue dotted line). PMFD output electrical spectrum (c) without and (d) with an OBPF inserted before the photodetector.

the SL free running power. Referring to Fig. 2(a), the injection light from the ML consists of several frequency components. Since the carrier and the first order lower sideband are the two frequency components that are close to the SL, the SL is mainly interacted with these two frequency components. Hence there are two sets of detuning frequency and injection strength. They can be obtained from the frequency and power of the SL relative to the ML carrier (f_{i1}, ξ_1) and the ML first order lower sideband (f_{i2}, ξ_2). By designing the detuning frequencies and the injection strengths, the SL can be oscillated in the period-two (P2) state. This results in the regeneration of the injection light and the generation of new subharmonic frequency components, at the SL output [17]. The new subharmonic frequency components generated by the SL oscillating in the P2 state are located at an integer multiple of a subharmonic frequency, which is half of the difference between the carrier frequency and the first order lower sideband frequency, i.e., $f_{RF}/2$, away from the injection light frequency. Hence the output electric field of the optically injected SL operating in the P2 state can be written as

$$\begin{aligned} E_{o,SL}(t) = E_{in}\sqrt{t_{ff}}e^{j\omega_c t}\Big[&A_{-2.5}e^{-j(2.5\omega_{RF}t-\theta_{-2.5})} \\ &+ A_{-2}e^{-j(2\omega_{RF}t-\theta_{-2})} \\ &+ A_{-1.5}e^{-j(1.5\omega_{RF}t-\theta_{-1.5})} + A_{-1}e^{-j(\omega_{RF}t-\theta_{-1})} \\ &+ A_{-0.5}e^{-j(0.5\omega_{RF}t-\theta_{-0.5})} + A_0e^{j(\theta_0)} \\ &+ A_{0.5}e^{j(0.5\omega_{RF}t+\theta_{0.5})} + A_1e^{j(\omega_{RF}t+\theta_1)} \\ &+ A_{1.5}e^{j(1.5\omega_{RF}t+\theta_{1.5})} + A_2e^{j(2\omega_{RF}t+\theta_2)} \\ &+ A_{2.5}e^{j(2.5\omega_{RF}t+\theta_{2.5})}\Big] \end{aligned} \tag{2}$$

where $A_{n/2}$ and $\theta_{n/2}$ are the amplitude and phase of the optical frequency component at $f_c \pm nf_{RF}/2$ respectively. Fig. 2(b) shows the output optical spectrum of the optically injected SL operating in the P2 state. Note that the frequency components that are close to the SL free running frequency have higher amplitude than those away from the SL free running frequency [17]. More importantly, two adjacent frequency components are

separated by f_{RF}/2. Beating of these frequency components at the photodetector generates a 1/2 frequency component at f_{RF}/2 together with its harmonic components at f_{RF}, 3f_{RF}/2, 2f_{RF}, etc. This can be seen in Fig. 2(c).

In order to suppress the harmonic components, a tunable optical bandpass filter (OBPF) is inserted before the photodetector as shown in Fig. 1. The bandwidth and the centre frequency of the optical filter are designed to pass two frequency components at f_c-f_{RF} and f_c-0.5f_{RF}, which are close to the SL free running frequency and have high amplitudes, while suppressing other frequency components. The electric filed at the output of the tunable OBPF is given by

$$\begin{aligned} E_{o,filter}(t) = E_{in}\sqrt{t_{ff}}e^{j\omega_c t}\Big[&\sqrt{\gamma_{-1.5}}A_{-1.5}e^{-j(1.5\omega_{RF}t-\theta_{-1.5})} \\ &+A_{-1}e^{-j(\omega_{RF}t-\theta_{-1})} \\ &+A_{-0.5}e^{-j(0.5\omega_{RF}t-\theta_{-0.5})}+\sqrt{\gamma_0}A_0e^{j(\theta_0)}\Big] \end{aligned} \tag{3}$$

Since the magnitude response of a tunable OBPF has a finite edge roll-off, the frequency components at f_c-3f_{RF}/2 and f_c, which are next to the two wanted frequency components, will leak through the optical filter. The amount of suppression introduced by the tunable OBPF to these unwanted frequency components are represented by $\gamma_{-1.5}$ and γ_0, which are included in (3). The output of the tunable OBPF is connected to a photodetector. The photocurrent generated by the photodetector can be obtained from (3) and is given by

$$\begin{aligned} I_o(t) = 2\Re P_{in}t_{ff}\,[&\sqrt{\gamma_0}A_0A_{-0.5}\cos(0.5\omega_{RF}t+\theta_{-0.5}-\theta_0) \\ &+A_{-0.5}A_{-1}\cos(0.5\omega_{RF}t+\theta_{-1}-\theta_{-0.5}) \\ &+\sqrt{\gamma_{-1.5}}A_{-1}A_{-1.5}\cos(0.5\omega_{RF}t+\theta_{-1.5}-\theta_{-1}) \\ &+\sqrt{\gamma_{-1.5}}A_{-0.5}A_{-1.5}\cos(\omega_{RF}t+\theta_{-1.5}-\theta_{-0.5}) \\ &+\sqrt{\gamma_0}A_0A_{-1}\cos(\omega_{RF}t+\theta_{-1}-\theta_0)] \end{aligned} \tag{4}$$

where $\Re$ is the photodetector responsivity and P_{in} is the CW light power into the phase modulator. (4) shows the output of the PMFD consists of the frequency divided signal at f_{RF}/2 and a suppressed harmonic component at f_{RF}. The proposed optically injected semiconductor laser based PMFD output electrical spectrum is shown in Fig. 2(d). In an ideal case where the unwanted frequency components at f_c-3f_{RF}/2 and f_c are fully eliminated by the OBPF, i.e., $\gamma_{-1.5} = \gamma_0 = 0$, only a divide-by-two signal is present at the PMFD output.

Note that, in the proposed PMFD, the two optical frequency components that interact with the SL are the optical carrier and the first order lower sideband. They are generated by the same laser source and hence they are correlated. This is different to using two independent laser sources for dual-beam optical injection [19]. Hence the frequency divided signal at the output of the proposed optically injected semiconductor laser based PMFD is stable and has a narrow linewidth [20]. The proposed PMFD only needs an optical circulator, a DFB laser and a tunable OBPF in a microwave photonic link formed by a laser, an optical phase modulator and a photodetector. It does not require any electrical component. Using an optical phase modulator for RF signal modulation has the advantages of bias free and lower loss compared to an intensity modulator that is used in majority of the reported PMFDs. Until now, there are only two reports on PMFDs that have the ability to suppress the harmonic components [9], [10]. They are based on the regenerative technique implemented using an OEO loop. They both requires four electrical components, which are a microwave amplifier, a phase shifter, a bandpass filter and a power splitter. The electrical bandpass filter, which has a fixed magnitude response, limits the operating frequency range of these PMFDs.

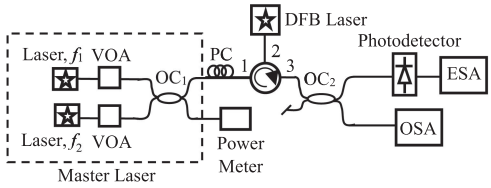

Fig. 3. Experimental setup for investigating P2 oscillation in a dual-beam optically injected DFB laser.

The proposed PMFD should find applications in phase-locked loops (PLLs), frequency synthesisers, phase shift keying (PSK) modulators and demodulators, and so on. In PLLs, a frequency divider is used to reduce a voltage control oscillator (VCO) output signal frequency [21]. The frequency divided signal is fed back to a phase detector, which produces an error signal proportional to the phase difference between the PLL input signal and the frequency divided signal. The error signal is injected into the VCO to alter the output signal phase. This process ensures the output signal phase is locked to the phase of the input signal. A frequency divider can also be used as a phase rotator in a PSK modulator [22], and together with a comparator to recover the carrier in a PSK demodulator [23].

III. Period-Two Oscillation

Since the proposed PMFD is operated based on P2 oscillation in a semiconductor laser, it is important to investigate the setting of the system parameters required to ensure the laser is oscillating in the P2 state for different input RF signal frequencies. Referring to the PMFD structure shown in Fig. 1, the system parameters that can be controlled are the CW light power, and the SL free running power and frequency. An experiment was set up as shown in Fig. 3 to design these parameters so that frequency division can be realised over a wide input RF signal frequency range. The setup consists of two tunable laser sources (Santec WSL-100 and Keysight N7711A). The two tunable lasers generated two different-frequency CW light at $f_1 = 193.491$ THz and $f_2 = 193.512$ THz. They passed through variable optical attenuators (VOAs) and were combined via a 2×2 50:50 optical coupler (OC_1). The average optical power measured on an optical power meter at an output of OC_1 was 5.5 dBm. Another output of OC_1 was connected to a polarisation controller (PC), which was adjusted to achieve maximum injection efficiency. This was followed by an optical circulator, and a 1550 nm DFB laser, which was used as a SL. Fig. 4(a) shows the optical

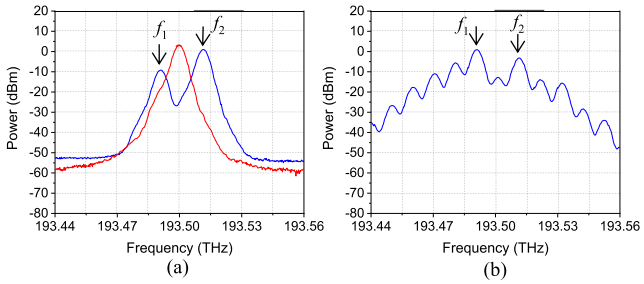

Fig. 4. (a) Optical spectrums of the two injection light beams with 20.46 GHz frequency separation (blue line) and the free running SL (red line). (b) Output optical spectrum of the SL when it is oscillating in the P2 state. The SL forward bias current is 36.2 mA.

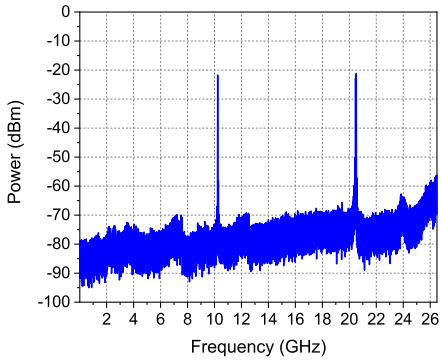

Fig. 5. Output electrical spectrum when the SL is oscillating in the P2 state.

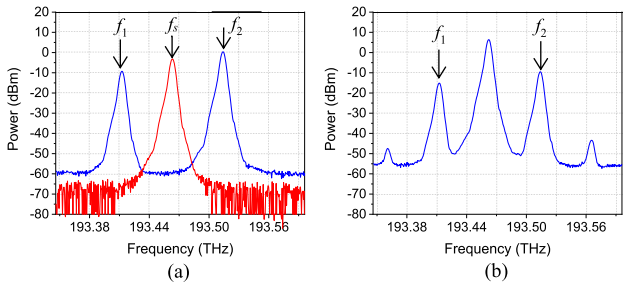

Fig. 6. (a) Optical spectrums of the two injection light beams with 101.31 GHz frequency separation (blue line) and the free running SL (red line). (b) Output optical spectrum of the SL when it is oscillating in the P2 state. The SL forward bias current is 80 mA.

spectrum measured on an optical spectrum analyser (OSA) at Port 2 of the optical circulator. The two frequency components shown in Fig. 4(a) are the two injection light beams. They represent the carrier and the first order lower sideband produced by the phase modulator in the proposed PMFD. They have 20.46 GHz frequency separation and 10 dB power difference, which correspond to a 20.46 GHz input RF signal and a modulation index of 0.6 in the proposed PMFD. The output of the DFB laser was routed from Port 2 to Port 3 of the optical circulator. A 2×2 50:50 optical coupler (OC_2) was employed after the circulator to enable simultaneous monitoring the SL output in both optical and electrical domain via an OSA and a photodetector followed by an electrical signal analyser (ESA) (Keysight N9000A).

The SL free running power and frequency can be controlled by adjusting the forward bias current and the temperature via a laser diode driver (Newport 505B) and a temperature controller (Newport 350B) respectively, connected to the DFB laser. The SL temperature was fixed at 24.7 °C. The SL forward bias current was adjusted until the subharmonic frequency components appear in the SL output optical spectrum as shown in Fig. 4(b). It can be seen from the figure that, in addition to the two original injection light beams, new frequency components at $n(f_2\text{-}f_1)/2$ away from the two light beams are generated where n is an integer. This indicates the SL is oscillating in the P2 state. The red line in Fig. 4(a) shows the corresponding SL free running spectrum, which was measured when there was no injection light into the SL. As shown, the SL free running frequency is 193.50 THz, which is in between the two injection light beams. The electrical spectrum measured on the ESA after the photodetector is shown in Fig. 5. This shows there are two electrical frequency components, which are located at $(f_2\text{-}f_1)/2 =$ 10.23 GHz and $f_2\text{-}f_1 = 20.46$ GHz. They were formed by beating of the optical frequency components shown in Fig. 4(b), at the photodetector.

The frequency separation of the two injection light beams was increased from 20.46 GHz to 101.31 GHz. This is shown by the blue line in Fig. 6(a). The figure also shows the powers of the two injection light beams are the same as that shown in Fig. 4(a). The SL temperature was 25 °C. By adjusting the SL forward bias current to 80 mA, the subharmonic frequency components at $(f_2\text{-}f_1)/2 = 50.655$ GHz away from the two light beams were generated. This can be seen from the SL output spectrum shown in Fig. 6(b). This indicates that the SL is oscillating in the P2 state. Since the ESA used in the experiment only has a 26.5 GHz bandwidth, the output electrical frequency components generated by the beating of the optical frequency components shown in Fig. 6(b) at the photodetector could not be measured. Nevertheless, the generation of new optical frequency components when the two injection light beams have 101.31 GHz frequency separation shows P2 oscillation bandwidth can be over 100 GHz. It was found from the experiment that, the SL current is the only system parameter that needs to be adjusted to ensure the SL is operating at the P2 state as the frequency separation between the two injection light beams changes. This indicates that, for the proposed PMFD, by simply adjusting the SL current, a frequency divided signal can be generated for different input RF signal frequencies.

IV. Experimental Results

The proposed optically injected semiconductor laser based PMFD was set up experimentally. The setup was similar to that shown in Fig. 3 except only one tunable laser source (Keysight N7711A) was employed. The CW light generated by the laser source was launched into an optical phase modulator (EOSpace PM-0S5-20) via a PC. The phase modulator was driven by a 16 GHz RF signal from a microwave signal generator (Analog Devices HMC-T2220). The RF phase modulated optical signal passed through a 2×2 50:50 optical coupler (OC_1) followed by another PC and was routed from Port 1 to Port 2 of the optical

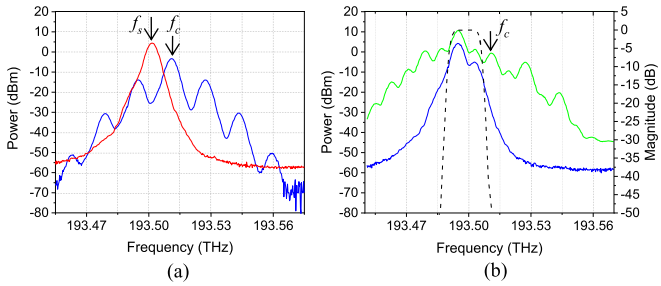

Fig. 7. (a) Optical spectrums of the ML when the input RF signal frequency is 16 GHz (blue line) and the free running SL (red line). (b) Optical spectrum before (green line) and after (blue line) the OBPF, and OBPF magnitude response (black dashed line).

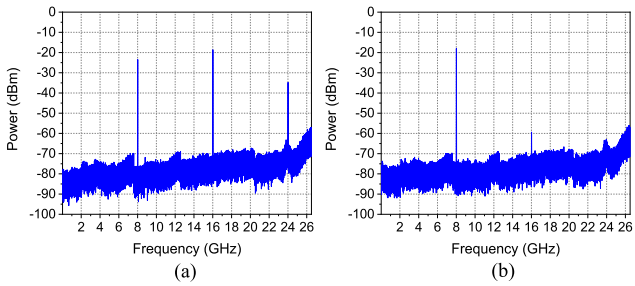

Fig. 8. Output electrical spectrum of the proposed PMFD (a) without and (b) with an OBPF inserted before the photodetector. The average optical power into the photodetector is 5.7 dBm. The ESA has a resolution bandwidth of 510 kHz and a video bandwidth of 51 kHz.

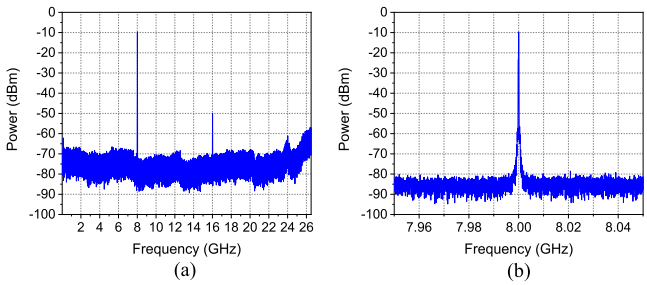

Fig. 9. Frequency divider output electrical spectrum when the average optical power into the photodetector is 10 dBm. The spectrum measured in (a) a wide 26 GHz span with a 510 kHz resolution bandwidth and a 51 kHz video bandwidth and (b) a 100 MHz span centred at 8 GHz with a 100 kHz resolution bandwidth and a 10 kHz video bandwidth.

circulator. Note that the performance of the optically injected semiconductor laser is dependent on the polarisation state of the injection light. Therefore, the PC at the phase modulator output was adjusted to achieve maximum injection efficiency. In practice, the PCs used in the experiment can be avoided by using polarisation maintaining components between the laser source and the SL. The same DFB laser as the one that was used to investigate P2 oscillation, was connected to Port 2 of the optical circulator. It was employed as the SL. The optical circulator output Port 3 was connected to an erbium-doped fibre amplifier (EDFA) followed by a tunable OBPF (Alnair Lab BVF-300CL). The optical signal at the filter output was detected by a photodetector.

The power of the 16 GHz input RF signal was adjusted to 10.7 dBm so that modulation index was 0.56. This results in a 10 dB power difference between the optical carrier and the first order lower sideband. This is the same as the power difference between the two injection light beams in the dual-beam optically injected semiconductor laser experiment given in the previous section. The average optical power after OC_1 was 5.5 dBm, which is also the same as that used in the dual-beam optically injected semiconductor laser experiment. The blue line in Fig. 7(a) shows the injection light spectrum, which was measured at Port 2 of the optical circulator. The SL temperature was fixed at 24.7 °C while the SL forward bias current was increased until P2 oscillation occurred. The SL output spectrum for a 32 mA current is shown by the green line in Fig. 7(b). This shows a SL current of 32 mA results in P2 oscillation, which is close to that obtained using two injection light beams when the two systems were operated under a similar condition. As shown, the first order lower sideband and its adjacent new frequency components generated by P2 oscillation have high amplitudes. Therefore the passband of the tunable OBPF was designed to select these two frequency components. The optical spectrum after the tunable OBPF is shown by the blue line in Fig. 7(b). The free running SL spectrum when the SL was operated at 24.7 °C and 32 mA forward bias current, is shown by the red line in Fig. 7(a). It can be seen from the figure that the SL free running frequency is 193.50 THz and is between the carrier and the first order lower sideband of the injection light. This situation is the same as the dual-beam optically injected semiconductor laser experiment presented in Section III. Two sets of detuning frequencies and injection strengths can be obtained from the frequency and power of the ML carrier and first order lower sideband relative to that of the free running SL. They are $(f_{i1}, \xi_1) = (9.24\ \text{GHz}, 0.411)$ and $(f_{i2}, \xi_2) = (-6.74\ \text{GHz}, 0.122)$.

Fig. 8(a) and 8(b) show the output electrical spectrums of the frequency divider without and with the tunable OBPF inserted before the photodetector. They were measured on an ESA connected to the photodetector output. In both cases, the average optical power into the photodetector was 5.7 dBm. Fig. 8(a) shows, without using an optical filter, the amplitude of the harmonic at 16 GHz is higher than that of the frequency divided signal at 8 GHz. It can be seen from Fig. 8(b) that, with the use of an optical filter to select only two frequency components from the SL oscillating in the P2 state, the harmonic at 16 GHz is suppressed to 41.4 dB below the 1/2 frequency component at 8 GHz. The figure also shows the higher order harmonics are suppressed to below the system noise floor. An over 41 dB suppression in the harmonic components is higher than that obtained using the PMFDs presented in [9] and [10]. The EDFA gain was adjusted to increase the average optical power into the photodetector to 10 dBm. This increases the power of the 1/2 frequency component at 8 GHz to -9.7 dBm as shown in Fig. 9. Fig. 9(b) shows the frequency divider output electrical spectrum measured in a 100 MHz span centred at 8 GHz. Unlike the PMFDs implemented using the regenerative technique [11], there are no spur peaks around the 1/2 frequency component. In addition, over 70 dB SNR in a 100 kHz noise bandwidth is obtained. The experimental results shown in Fig. 9 indicate the conversion efficiency of the PMFD, which is the ratio of the

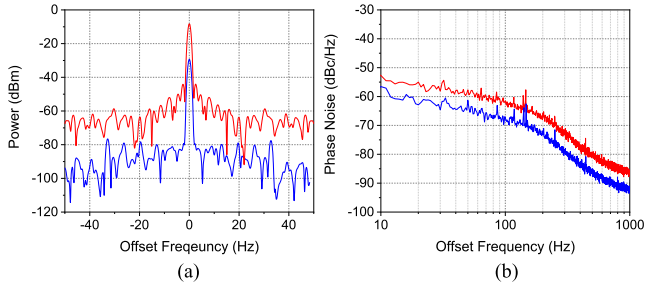

Fig. 10. (a) Electrical spectrums and (b) phase noise spectrums of the 16 GHz RF signal into the PMFD (red line) and the 8 GHz frequency divided signal at the output of the PMFD (blue line).

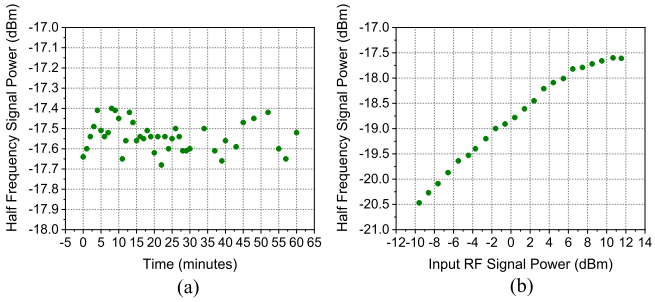

Fig. 11. Power of the half frequency component at 8 GHz (a) measured over 60 minutes and (b) for different RF signal powers into the frequency divider.

output frequency divided signal power to the input RF signal power, is around -20 dB. This shows the PMFD has around 20 dB loss. The loss is mainly due to the electrical-optical-electrical conversion process. It can be reduced by increasing the average optical power into the photodetector or using an electrical amplifier, which is used in all PMFDs implemented using an OEO loop, to amplify the frequency divided signal.

Fig. 10(a) shows the 16 GHz RF signal into the PMFD and the 8 GHz frequency divided signal at the output of the PMFD measured on the ESA with a 100 Hz span and a 20 dB attenuator at the spectrum analyser input. The phase noise of the PMFD input and output RF signals were measured on the ESA using the method described in [24], [25]. As can be seen in Fig. 10(b), the phase noise of the input 16 GHz RF signal at a 100 Hz offset frequency is -61.5 dBc/Hz, which is close to that stated in the datasheet of the microwave signal generator (Analog devices HMC-T2220) used in the experiment. The figure also shows the phase noise of the 8 GHz frequency divided signal is -67.2 dBc/Hz. This shows a 5.7 dB improvement in the phase noise performance, which agrees with the theoretically predicted phase noise improvement of $10\log_{10}(2^2) = 6.0$ dB.

The proposed PMFD output stability was examined by measuring the power of the 1/2 frequency component at the frequency divider output over a one-hour period. As shown in Fig. 11(a), the 1/2 frequency component has less than 0.3 dB power fluctuation during the measurement period. No change in the frequency of the 1/2 frequency component was observed for an hour. This indicates that the PMFD has a stable performance. Next, an experiment was conducted to determine the input RF signal power range in which a stable 1/2 frequency component

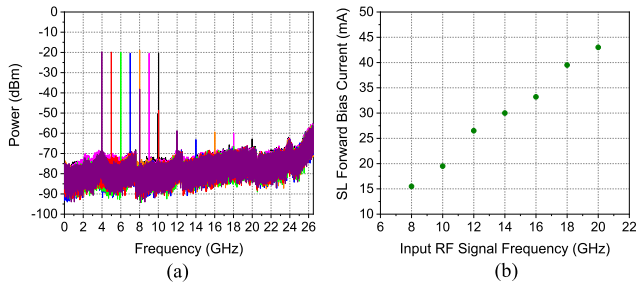

Fig. 12. (a) Output electrical spectrum of the proposed PMFD when the input RF signal frequency is 8 GHz (purple line), 10 GHz (red line), 12 GHz (green line), 14 GHz (blue line), 16 GHz (orange line), 18 GHz (pink line) and 20 GHz (black line). (b) SL forward bias currents required for a different-frequency RF signal into the frequency divider to generate a 1/2 frequency component.

can be generated at the frequency divider output. This was done by changing the power of the 16 GHz RF signal into the PMFD while fixing all system parameters. It was found that, when the input RF signal power is between -9.6 dBm to 11.5 dBm, the 1/2 frequency component generated by the PMFD has a stable amplitude and frequency. A -9.6 dBm to 11.5 dBm input RF signal power range corresponds to a modulation index range of 0.05 to 0.61 for the optical phase modulator used in the experiment has a switching voltage of 6.1 V at 16 GHz. The power difference between the carrier and the first order lower sideband is ranging from around 9 dB to 29 dB in this modulation index range. Fig. 11(b) shows the power of the 1/2 frequency component increases as the input RF signal power changes from -9.6 dBm to 11.5 dBm. The result shows the PMFD can be operated over a wide input RF power range.

The ability of the proposed PMFD to operate at different input RF signal frequencies was investigated. Fig. 12(a) shows the frequency divider output electrical spectrums for different input RF signal frequencies from 8 GHz to 20 GHz. They were obtained by adjusting the SL forward bias current. The modulation index was fixed at 0.56 for different input RF signal frequencies. This shows frequency division with large harmonic suppression can be obtained for different input RF signal frequencies. The power of the frequency divided signal remains almost the same at around -20 dBm, as the input RF signal frequency changes. Compared to [16], the lower limit of the optically injection semiconductor laser based PMFD operating frequency range was improved from 12 GHz to 8 GHz. This was obtained by optimising the injection strengths and the detuning frequencies to ensure the SL free running frequency is between the frequencies of the ML carrier and first order lower sideband even for an 8 GHz input RF signal. Fig. 12(a) shows the amount of harmonic component suppression reduces to around 20 dB when the input RF signal frequency is 8 GHz. This is because the unwanted optical frequency components at f_c and f_c-1.5f_{RF} are closer to the tunable OBPF passband as the input RF signal frequency reduces. This results in the unwanted optical frequency components cannot be largely suppressed by the tunable OBPF, which leads to the increase of the amplitude of the harmonic components generated after photodetection. Fig. 12(b) shows the SL forward bias current required to realise

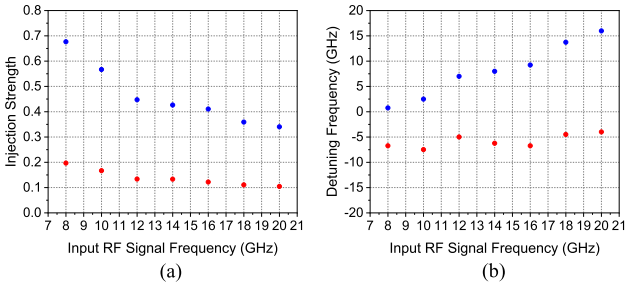

Fig. 13. Required (a) injection strengths and (b) detuning frequencies, obtained from the powers and frequencies of the SL together with the ML carrier (blue dots) and first order lower sideband (red dots), for the SL to oscillate in the P2 state versus input RF signal frequency.

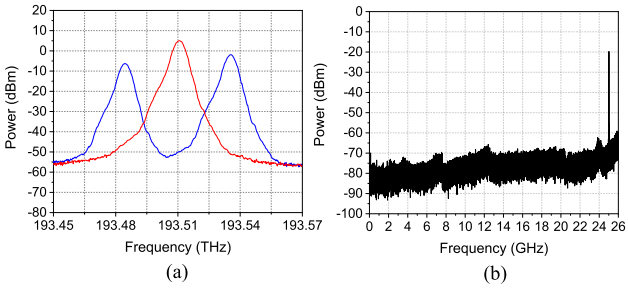

Fig. 14. (a) Optical spectrums of the two injection light beams with around 50 GHz frequency separation (blue line) and the free running SL (red line). (b) Output electrical spectrum when the SL is oscillating in the P2 state.

half frequency division for different input RF signal frequencies. As shown, the higher the input RF signal frequency, the larger the SL forward bias current is needed. Changing the SL forward bias current alters both the SL free running power and frequency. This consequently alters the injection strengths and the detuning frequencies. The powers and frequencies of the free running SL together with that of the ML carrier and first order lower sideband were used to obtain the injection strengths and the detuning frequencies. Fig. 13 shows the two injection strengths reduce and the two detuning frequencies increase as the input RF signal frequency increases, in order to ensure the SL is oscillating in the P2 state to realise frequency division operation. Fig. 13(b) shows, when the input RF signal frequency is 8 GHz, the SL free running frequency is close to the ML carrier frequency. According to the figure, an input RF signal frequency of below 8 GHz will require a smaller detuning frequency and hence the SL free running frequency will be outside the ML carrier and first order lower sideband frequency range. Therefore, a frequency divided signal at a frequency of less than 4 GHz cannot be generated by only adjusting the SL forward bias current.

Due to the bandwidth limitation of the microwave signal generator used in the experiment, frequency division operation for an input RF signal with a frequency above 20 GHz cannot be demonstrated. To show the proposed PMFD has the potential to realise 1/2 frequency division operation for a 50 GHz input RF signal, the ML as shown in the dashed box in Fig. 3 was set up. The two injection light beams from the ML had around 50 GHz frequency separation. They were launched into the SL via an optical circulator. Fig. 14(a) shows the optical spectrums of the injection light from the ML and the free running SL when the SL is oscillating in P2 state under optical injection. Optical frequency components with a frequency separation of around 25 GHz were generated by the SL. After photodetection, an RF signal at 25.02 GHz, which is half the frequency separation of the two injection light beams, was obtained as shown in Fig. 14(b). Note that P2 oscillation in the DFB laser when the two injection light beams have a frequency separation of 101.31 GHz, was also demonstrated in Section III. Hence the proposed PMFD is expected to be able to operate over a very wide frequency range with the maximum operating frequency only limited by the optical phase modulator bandwidth.

V. Conclusion

An all-optical PMFD has been proposed and experimentally demonstrated. An RF phase modulated optical signal is injected into an off-the-shelf DFB laser. The DFB laser is operating in the P2 oscillation state by adjusting the laser forward bias current. In this way, new optical frequency components, which are in the midpoint of the injection light frequency components, are generated. Using a tunable OBPF to select two frequency components at f_c-0.5f_{RF} and f_c-f_{RF} while blocking other frequency components, a frequency divided signal with large harmonic suppression is obtained. This solves the problem of many reported PMFDs that generate high harmonic components, which distorts the frequency divider output signal. The proposed PMFD does not require any electrical component. It has a simpler structure than the PMFDs implemented using the regenerative technique or the injection locking technique. Using an optical phase modulator for RF signal modulation has the advantage of no bias drift problem, compared to many reported PMFDs that use an intensity modulator for RF signal modulation. P2 oscillation in an off-the-shelf DFB laser was demonstrated experimentally using two tunable laser sources with a 101.31 GHz frequency separation. This shows, the proposed PMFD that is operated based on a SL oscillating in the P2 state, can have a very wide operating frequency range. Experimental results demonstrated half frequency division for an input RF signal frequency range of 8 GHz to 20 GHz, by adjusting the SL forward bias current. The output frequency divided signal was stable for a wide input RF signal power range of -9.6 dBm to 11.5 dBm. Over 40 dB harmonic suppression and over 70 dB SNR in a 100 kHz noise bandwidth were obtained for a 16 GHz RF signal into the PMFD.

References

[1] T. Nagatsuma and Y. Kado, "Microwave photonic devices and their applications to communications and measurements," *PIERS Online*, vol. 4, no. 3, pp. 376–340, 2008.

[2] M. Sans, C. Renaud, and J. E. Mitchell, "Opto-electronic cross-phase tuneable system based on cascaded intensity modulators," in *Proc. Int. Topical Meeting Microw. Photon.*, 2017, pp. 1–4.

[3] S. Pan and Y. Zhang, "Microwave photonic radars," *J. Lightw. Technol*, vol. 38, no. 19, pp. 5450–5484, Oct. 2020.

[4] R. A. Minasian, E. H. W. Chan, and X. Yi, "Microwave photonic signal processing," *Opt. Exp.*, vol. 21, no. 19, pp. 22918–22936, 2013.

[5] J. P. Yao, "Microwave photonics," *J. Lightw. Technol.*, vol. 27, no. 3, pp. 314–335, Mar. 2009.

[6] Y. Xu et al., "Injection-locked millimeter wave frequency divider utilizing optoelectronic oscillator based optical frequency comb," *IEEE Photon. J.*, vol. 11, no. 3, Jun. 2019, Art. no. 5501508.
[7] Y. Meng, T. Hao, W. Li, N. Zhu, and M. Li, "Microwave photonic injection locking frequency divider based on a tunable optoelectronic oscillator," *Opt. Exp.*, vol. 29, no. 2, pp. 684–691, 2021.
[8] S. Liu, K. Lv, J. Fu, L. Wu, W. Pan, and S. Pan, "Wideband microwave frequency division based on an optoelectronic oscillator," *IEEE Photon. Technol. Lett.*, vol. 31, no. 5, pp. 389–392, Mar. 2019.
[9] H. Zhou et al., "Broadband two-thirds photonic microwave frequency divider," *Electron. Lett.*, vol. 55, no. 21, pp. 1141–1143, 2019.
[10] H. Zhou, N. Zhu, S. Liu, D. Zhu, and S. Pan, "One-third optical frequency divider for dual-wavelength optical signals based on an optoelectronic oscillator," *Electron. Lett.*, vol. 56, no. 14, pp. 727–729, 2020.
[11] S. Duan et al., "Photonic-assisted regenerative microwave frequency divider with a tunable division factor," *J. Lightw. Technol.*, vol. 38, no. 19, pp. 5509–5516, Oct. 2020.
[12] W. Zhang, J. Sun, J. Wang, X. Zhang, and D. Huang, "Optical clock division based on dual-wavelength mode-locked semiconductor fiber ring laser," *Opt. Exp.*, vol. 16, no. 15, pp. 11231–11236, 2008.
[13] A. E. Kelly, R. J. Manning, A. J. Poustie, and K. J. Blow, "All-optical clock division at 10 and 20 GHz in a semiconductor optical amplifier based nonlinear loop mirror," *Electron. Lett.*, vol. 34, no. 13, pp. 1337–1339, 1998.
[14] S. Chan and J. Liu, "Microwave frequency division and multiplication using an optically injected semiconductor laser," *IEEE J. Quantum Electron.*, vol. 41, no. 9, pp. 1142–1147, Sep. 2005.
[15] M. Zhang, T. Liu, A. Wang, J. Zhang, and Y. Wang, "All-optical clock frequency divider using Fabry–Perot laser diode based on the dynamical period-one oscillation," *Opt. Commun.*, vol. 284, no. 5, pp. 1289–1294, 2011.
[16] H. Chen and E. H. W. Chan, "Ultra-simple all-optical microwave frequency divider," *IEEE Photon. Technol. Lett.*, vol. 34, no. 4, pp. 219–222, Feb. 2022.
[17] X. Qi and J. Liu, "Dynamics scenarios of dual-beam optically injected semiconductor lasers," *IEEE J. Quantum Electron.*, vol. 47, no. 6, pp. 762–769, Jun. 2011.
[18] Y. Liao, J. Liu, and F. Lin, "Dynamical characteristics of a dual-beam optically injected semiconductor laser," *IEEE J. Sel. Topics Quantum Electron.*, vol. 19, no. 4, Jul./Aug. 2013, Art. no. 1500606.
[19] Y. Juan and F. Lin, "Photonic generation of broadly tunable microwave signals utilizing a dual-beam optically injected semiconductor laser," *IEEE Photon. J.*, vol. 3, no. 4, pp. 644–650, Aug. 2011.
[20] Y. H. Hung and S. K. Hwang, "Photonic microwave stabilization for period-one nonlinear dynamics of semiconductor lasers using optical modulation sideband injection locking," *Opt. Exp.*, vol. 23, no. 5, pp. 6520–6532, 2015.
[21] M. Bomford, "Selection of frequency dividers for microwave PLL applications," *Microw. J.*, vol. 33. no. 11, pp. 159–167, 1990.
[22] Z. Ji, S. Zargham, and A. Liscidini, "Low-power QPSK transmitter based on an injection-locked power amplifier," in *Proc. IEEE 44th Eur. Solid State Circuits Conf.*, 2018, pp. 134–137.
[23] Z. He, D. Nopchinda, T. Swahsn, and H. Zirath, "A 15-Gb/s 8-PSK demodulator with comparator-based carrier synchronization," *IEEE Trans. Microw. Theory Techn.,* vol. 63, no. 8, pp. 2630–2637, Aug. 2015.
[24] Q. Wang, H. Rideout, F. Zeng, and J. Yao, "Millimeter-wave frequency tripling based on four-wave mixing in a semiconductor optical amplifier," *IEEE Photon. Technol. Lett.*, vol. 18, no. 23, pp. 2460–2462, Dec. 2006.
[25] C. Huang, H. Chen, and E. H. W. Chan, "Microwave photonic frequency tripler based on an integrated dual-parallel modulator structure," *IEEE Photon. J.*, vol. 9, no. 5, Oct. 2017, Art. no. 7204010.